Soft Matter

RSC Publishing

PAPER

View Article Online
View Journal | View Issue

FtsZ protein on bilayer membranes: effects of specific lateral bonds

Cite this: *Soft Matter*, 2013, **9**, 6072

Pablo González de Prado Salas,[a] Mario Encinar,†[b] Marisela Vélez[bc] and Pedro Tarazona*[ad]

We use a simple lattice model to explore the self-assembled structures of protein filaments. Monte Carlo simulations show polymorphic structures, formed by the competition between the bundling of filaments, their branching and the spontaneous curvature. In the top-down approach, typical of statistical physics, we compare the simulation results with experimental atomic force microscopy images of the bacterial protein FtsZ anchored on bilayer membranes. We identify the relevant aspects of the interactions between protein monomers, which are amplified as a collective effect of the whole system. From the perspective of soft-matter physics, the experimental system and its model representation provide an interesting example of living polymers with tunable interactions.

Received 26th February 2013
Accepted 29th April 2013

DOI: 10.1039/c3sm50590a

www.rsc.org/softmatter

1 Introduction

Protein and lipid bilayer membranes are the building blocks of the cellular structure and machinery. The biological selection of the proteins has optimized their interactions so that they may self-assemble into amazingly efficient structures required by the cell cycle. A huge effort is being made to unveil the complex molecular structure of proteins, from the genome to their folded structures. A complementary strategy, from the statistical physics point of view, is to develop simple coarse-grained models that reproduce the observed self-assembled structures. A few *relevant features* of the protein structure, enhanced by their *collective effects*, could then be identified as the essential part of their mutual interactions. In this paper we study the bacterial protein FtsZ,[1,2] the main component of the septal ring formed on the inner side of the bacterial membrane, which is crucial for the cell division process.[3–5] The self-assembled structures of FtsZ have been analyzed in controlled biomimetic experiments.[6] The globular protein monomers, with a diameter of 4.5 nm, form long filaments of length up to several microns that behave as supra-macromolecular living polymers (LPs),[7–9] *i.e.* the (longitudinal) bonds that form the filaments may be broken and remade, under the thermal fluctuations of the system, rather than being frozen after a polymerization reaction has been arrested. Atomic Force Microscopy (AFM) images of FtsZ filaments adsorbed onto mica surfaces[10] show complex structures and textures, evolving on a time scale of minutes. The filaments are flexible, with fluctuations around a spontaneous curvature;[11,12] they are broken and shuffled by the thermal fluctuations, characteristic of LP systems,[8] and they condensate into polymorphic bundles.

More recently, AFM images of FtsZ filaments have been obtained in biomimetic environments, with the protein on top of a lipid bilayer membrane,[13] and the observed patterns differ significantly from those with the protein on mica. The experimental evidence points to the relevance of the intrinsic properties of the membrane; the aggregates formed by the protein may be different on bilayers of different phospholipids (synthetic DOPC *versus* the mixture of polar phospholipids in the natural *E. coli* membrane).[14] It is also very relevant the way in which the protein is anchored to the membrane, either through a loose link with the membrane protein ZipA, or through FtsZ mutants designed to form a more specific anchoring. A particularly interesting version of this strategy locates a reactive cysteine in a FtsZ mutant to anchor the protein directly, and tightly, to specific lipid molecules.[14] The cysteine may be located at different positions on the surface of the FtsZ monomer, so that the relevance of the protein orientation may be explored. Fig. 1(a) and (c) show two observed structures for two different FtsZ mutants (Cys2 and Cys255) that are anchored to the *E. coli* bilayer membrane. The mutations are located in different positions in the protein: Cys2 is near the amino terminal domain and Cys 255 is near the carboxy terminal domain, which are located approximately

[a]*Departamento de Física Teórica de la Materia Condensada, Facultad de Ciencias, Universidad Autónoma de Madrid, E-28049 Madrid, Spain*

[b]*Instituto de Catálisis y Petroleoquímica, CSIC. C/Marie Curie, 2, E-28049, Madrid, Spain*

[c]*Instituto Madrileño de Estudios Avanzados en Nanociencia (IMDEA-Nanociencia), E-28049, Madrid, Spain*

[d]*Condensed Matter Physics Center (IFIMAC), Instituto de Ciencia de Materiales Nicolás Cabrera, Universidad Autónoma de Madrid, E-28049 Madrid, Spain. E-mail: pedro.tarazona@uam.es*

† Present address: Instituto de Microelectrónica de Madrid, CSIC. C/Isaac Newton 8 (PTM), E-28760 Tres Cantos, Madrid, Spain.

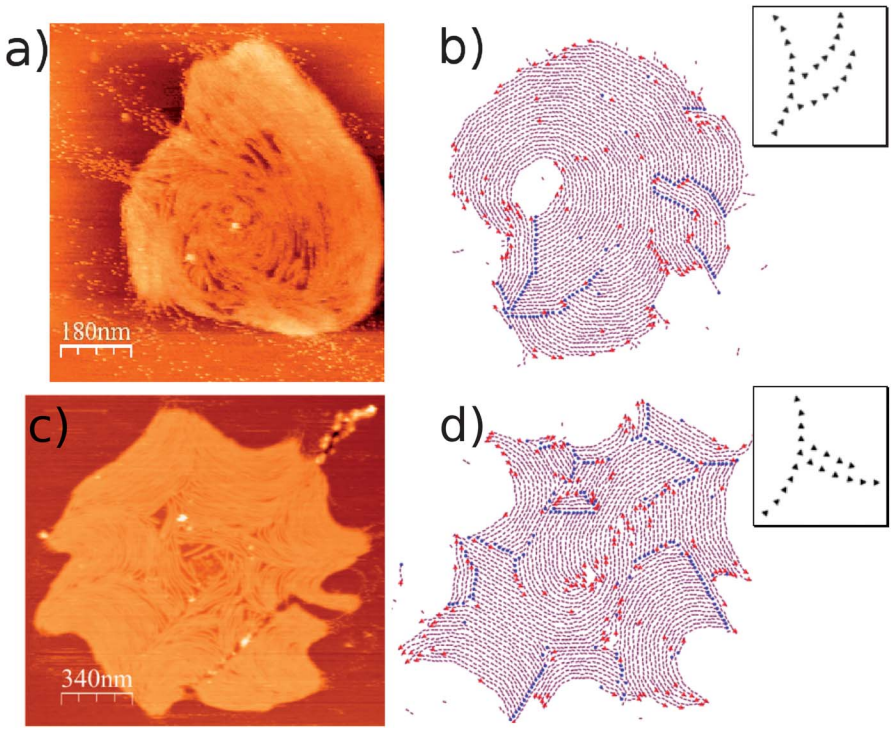

Fig. 1 AFM images of FtsZ protein mutants Cys2 (a) and Cys255 (c), anchored on *E. coli* Polar Extract bilayer membranes, are compared with snapshots of the lattice model (b–d) with the same interaction parameters, $(U_b,U_{sl},U_a,U_{+,}U_{-}) = (8,5.5,1.25,6,0)$ in kT units, and the two choices for the coupling between the spontaneous curvature and the trimeric bond, illustrated in the respective insets (and in Fig. 3). The circles (on-line blue) and triangles (red) give the extreme monomers for each filament.

180 degrees from each other. Therefore we assume that the proteins have, respectively, either the carboxy or the amino end oriented away from the lipid surface. Both AFM images are qualitatively different from those formed with the protein adsorbed on mica,[15] and we address here the question of how this new experimental information may be interpreted in terms of a model for the effective interactions between protein monomers.

Computer simulations with simplified models for FtsZ have been used over the last decade,[16–18] and the advances in the experimental techniques have provided the information to develop more detailed models.[11,15] In particular, the experimental results for FtsZ on mica were used to tune the interaction parameters of a fine-grained lattice model.[15] Despite the practical difficulty in quantifying the complex patterns and textures observed in the AFM images, it was shown that they could be qualitatively reproduced in terms of a minimal set of interaction parameters that represent the strong longitudinal bond along the filaments, the weaker lateral attraction between them and their spontaneous curvature. These parameters extract the relevant aspects of the extremely complex atomic structure of the protein[19] and the effects of the substrate. The (semi-)quantitative estimation of these parameters was done from the exploration of the global phase diagram of the lattice model, since the polymorphism observed in the AFM images could only be reproduced over a relatively small parametric region, in the boundary between regions with different stable structures.

We demonstrate here that the same approach may be used to reproduce the aggregation structures formed by FtsZ on bilayer membranes, and to extract from them some qualitative aspects of the effective interaction between the protein monomers, mediated by their anchoring to the membrane. We use an extension of the previous model, developed for FtsZ on mica,[15] and we incorporate the effects of a strong lateral bond (SLB) that produces branching filaments as observed in experiments with low protein coverage (Fig. 2(a) and (b)). Our results show the importance of the collective effects that could not be inferred from the detailed (atomistic) view of the interactions between three or four protein monomers. What really matters to form the observed structures is the coupling between the spontaneous curvature of the filaments and their branching topology, together with the flexibility and the LP character of the SLB, at a scale much larger than the monomers. We have only hints about the molecular origin of these SLB, and on the role of the lipid membrane to raise or modulate them,[14] since they do not seem to be needed to reproduce the structures of the protein on mica.[10] Also, it is an open question how these particular lateral interactions participate in the formation of the FtsZ ring *in vivo*. However, their prominent role in determining the shape of filament aggregates formed *in vitro* on lipid surfaces stresses the fact that the shape of the aggregates can be easily tuned by interactions other than the longitudinal bond between monomers. It is possible that FtsZ binding proteins found *in vivo* could use this plasticity to regulate their function inside the cell.

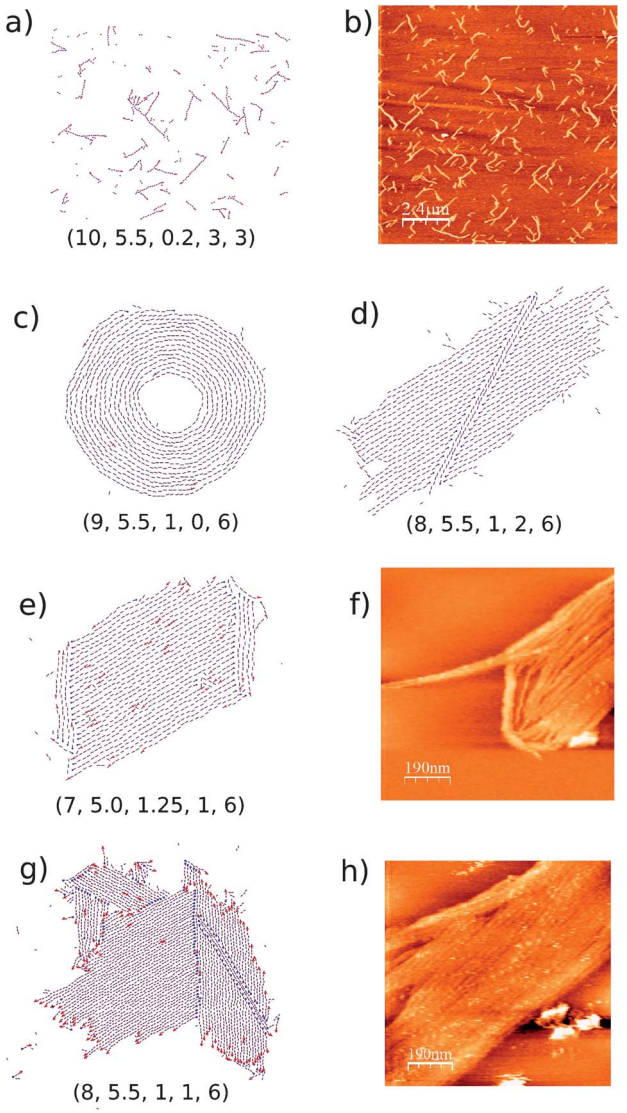

Fig. 2 (a) Snapshot of the model and (b) experimental AFM image for low protein coverage, with similar branching of the short filaments. (c–e) and (g) are typical aggregates formed in the lattice model with several sets of interaction parameters (U_b,U_{sl},U_a,U_-,U_+), in kT units. The circles (on-line blue) and triangles (red) give the starting and ending monomers for each filament. The AFM images (f and h) are taken for FtsZ mutant Cys2 on DOPC bilayer membranes.

2 Materials and methods

Protein purification and assay

Mutation and overexpression of mutant *E. coli* FtsZ are explained in ref. 14.

Preparation of EcFtsZ mutants anchored to planar lipid bilayers and AFM imaging

For a more thorough description of the experimental procedures see ref. 14. In brief, planar lipid bilayers on mica were formed by fusion of small unilamellar vesicles made of a mixture of *E. coli* polar lipids (EcPL) (Avanti Polar Lipids) and distearoyl *N*-(3-maleimido-1-oxopropyl)-L-phosphatidylethanolamine (DSPE-Mal, NOF Corporation). A 2 μM solution of the mutant protein was incubated on the formed bilayer (ratio of 1 : 5 linker lipid head to protein) for several hours to ensure complete coverage of the active surface. Atomic Force Microscopy (AFM) imaging was performed on the bilayer anchored FtsZ mutant in buffer after rinsing the excess protein in the presence of 5 mM GTP. AFM images were taken with a microscope from Nanotec Electrónica (Madrid, Spain) operated in the jump mode[20] in a liquid environment. The scanning piezo was calibrated using silicon calibrating gratings (NT-MDT, Moscow, Russia). Silicon nitride tips (Veeco) with a force constant of 0.05 Newton per m and 20 nm tip radius were used.

3 Lattice model and simulations

The lattice model introduced by Paez *et al.*[15] went beyond the coarse description of previous square-lattice models,[16–18] and it followed an approach similar to that of Sayar and Stupp[21] to describe flexible self-assembled filaments. A fine-grained triangular lattice, with a lattice space of about 1.5 nm, gives a geometrical resolution similar to that of the AFM images. The model was kept as simple as possible, using two dissimilar energy parameters, $U_b \gg U_a$, to represent the binding energy ($-U_b$) of protein monomers along the filament, and the weak lateral attraction ($-U_a$). The flexibility and preferential curvature of the filaments may be reproduced in terms of the energy parameters U_+ and U_-, to take into account the bending energy of the bond. The lattice space is smaller than the monomer size, with a set of 30 excluded neighbour sites. The attractive interactions are restricted to a crown of 42 sites, and the longitudinal axis of the monomers allowed having 24 orientations, that determine the formation of the strong longitudinal bond (LB). The analysis of the shapes of filaments and bundles in AFM images,[10,11] under different protein coverage of the mica substrate, provided a (semi-)quantitative fit for the model parameters to $\beta U_b \approx \beta U_+ = 10(\pm 2)$, $\beta U_a = 0.5(\pm 0.1)$, $\beta U_- = 0.5(\pm 0.5)$. Notice that the limited resolution of the experimental data precluded a more accurate fit, but still the similarity between the structures observed in the AFM images, and those in the MC snapshots of the lattice model, was quite remarkable. The protein interactions appear to be in a particularly interesting part of the generic phase diagram for the model, where the system shows large plasticity and polymorphism. In physical terms, these features were understood as the results of the thermodynamic balance between three basic cluster shapes named O, C and I. The I-clusters are rectangular 2D-nematic drops with the filaments aligned with the long sides. The C-clusters reflect the spontaneous curvature of the filaments, at the entropic cost of having a common head-to-tail orientation. The O-clusters are formed by rings and spirals, with very few open filament ends. Only over a small region of the parametric space in the model we find that these three basic clusters have similar free energies, so that they compete and form the complex polymorphic structures observed in the AFM images of FtsZ on mica.

Obviously, the precise numerical values of the interaction parameters should not be taken separately from the fine-grained lattice description, which was carefully chosen to

explore the model with Monte Carlo (MC) simulations. The shape and positions of the filaments are easily equilibrated through the MC trial moves that displace or rotate a monomer to a neighbour lattice site or orientation, without breaking the strong longitudinal bond.[15] The dynamics produced by these MC moves may be taken as a qualitative representation of the diffusive dynamics of the proteins on the substrate in the water bath.[22] The difference between the rapid kinetics of the filament shape and the slow thermal equilibration of the filament size is characteristic of living polymers,[8] and it is strongly represented in our model. With $\beta U_b \approx 8$–10, a move that breaks longitudinal bonds is accepted only once in every $\exp(\beta U_b) \sim 10^4$ MC trials. We have used long simulations (up to 10^9 MC steps) to sample the rare events in which the strong longitudinal bonds are broken.

The new feature included here is the presence of branching, which was apparently absent in the FtsZ filaments on mica, but observed when the protein is anchored with a specific orientation on a lipid bilayer (Fig. 2(a) and (b)). We include a new energy parameter U_{sl} in the model to describe a new pairwise interaction, weaker than the longitudinal bond but stronger than the isotropic lateral attraction. The SLB has free energy $-U_{sl}$, and it is formed when a pair of monomers has a specific relative orientation. We consider two alternative SLB branching structures, shown in Fig. 3, that only differ in the head-to-tail direction of the filaments, or equivalently, in the relative orientation of the spontaneous curvature of the filaments (both cases are sketched in Fig. 3).

If we assume that the molecular nature of the SLB is associated with the region with the acute angle of $\approx 60°$ (rather than with the $\approx 120°$ angle region), then in the configuration (a) the SLB would be formed between the inner side of a monomer and the outer side of the other monomer, while in the configuration (b) the SBL would be formed between the same (outer) side in both monomers. Notice that the AFM images do not give information on the orientation of the monomers, and the details of the filamentary structure are in the limit of the resolution. Any inference on the molecular nature of the interactions from the shape of the mesoscopic structures provides very valuable information, and we show here that the comparison between the AFM images and typical snapshots of our lattice model provides clear support for the presence of SLB and allows to discern between the two alternative configurations in Fig. 3. The FtsZ mutants Cys2 and Cys255 were selected to be anchored in nearly opposite orientations on the membrane, like turning the shapes up-side-down on the paper. The complex three dimensional asymmetry of the protein monomers, and their interaction with the lipid membrane below them, may change the effective interactions between the monomers under that change of their orientation. As presented in Fig. 1, the best (qualitative) representation of the experimental structures for the two mutants is obtained with the opposite choices for the geometrical configurations of the SLB.

To get the interaction parameters used in Fig. 1, we have run canonical ensemble Monte Carlo (MC) simulations, with a coarse search over the values of $(U_b, U_{sl}, U_a, U_+, U_-)$, and with the experience gained in the previous analysis for the protein on mica.[15] We have chosen $\beta U_b = 8$, at the lower limit of the previous range, to get relatively shorter filaments, and kept the same bending energy $\beta U_- = 0$ used for the protein on mica. The reported value $\beta U_+ = 6$ could be changed without a visible effect, as far as $U_+ \gg U_-$. Besides the inclusion of the new SLB, the main change in the interaction parameters of the model is that the (isotropic) lateral attraction U_a has to be significantly raised, from $\beta U_a \approx 0.5$ for mica to $\beta U_a \approx 1$–1.25 for the protein on the bilayer membrane, to reproduce the observed strong condensation of the protein, with very short and scarce isolated filaments and clusters. The strength of the new SLB was fixed to be around $\beta U_{sl} = 5.5 \pm 1$, and it is essential to reproduce the peculiar aspect of the experimental structures.

Relying on the qualitative aspect of the experimental images has proved to be the best procedure to fix the interaction parameters in the model. This method may seem too rough, and somehow arbitrary, since we are considering the qualitative shape and texture of the aggregates, without any attempt to quantify its geometrical aspects (size distribution of the filaments, number of lateral and SLB, mean curvature, *etc.*). A quantitative description of the aggregates in these terms may be easily obtained for the simulated model (see Table 1), but the resolution of the AFM does not allow a useful comparison with the MC results. However, the strong polymorphism of the system produces qualitative changes in the aggregates under small changes in the interaction parameters, and it allows good

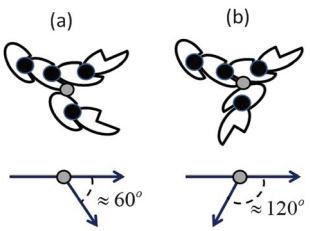

Fig. 3 Sketches for the two alternative configurations of the strong lateral bonds (SLB). The bottom shows the two alternatives in terms of the angle between the heads of the two filaments. The sketch in the top file gives (arbitrary) asymmetrical shapes to the monomers, to show how the tail-to-head direction along a filament is associated with the spontaneous curvature. Black circles represent the longitudinal bonds along each filament, while the grey circles indicate the specific SLB in each case.

Table 1 The number of filaments N_{fil}, their mean length L_{fil}, the number of strong lateral bonds N_{SL}, and the fraction of filaments with a strong lateral bond obtained in our lattice model with the interaction parameters used in the different frames of Fig. 4. To follow the tendencies with the interaction parameters, we give explicitly the structure of SLB (see Fig. 3) and the strength of the normal lateral bond βU_a in $kT \approx 0.6$ kcal mol^{-1} units

Frame	SLB	βU_a	N_{fil}	L_{fil}	N_{SL}	N_{SL}/N_{fil}
a1	(a) 60°	1	346	10.4	299	0.864
a2	(a) 60°	1	284	12.3	234	0.824
b1	(b) 120°	1	299	12.0	206	0.689
b2	(b) 120°	1	252	14.3	160	0.635
c1	(b) 120°	1.25	241	14.9	241	0.858
c2	(b) 120°	1.25	157	22.9	157	0.651

(semi-)quantitative tuning of the parameters based only on the qualitative aspect of the images. Fig. 2 is a typical show-gallery in which we play with small variations in the values of (U_b,U_{sl},U_a,U_+,U_-), and observe very different aggregates. The snapshot (a) corresponds to a low protein coverage and weak lateral attraction, so that the system is a mixture of short filaments that fluctuate in shape and size, the lateral attraction not being strong enough to produce their collective condensation. The effect of the SLBs is clearly reflected in the characteristic *Y* structures in which a filament meets another one with angles close to 60 or 120 degrees. Qualitatively similar structures are observed in AFM images taken under low protein coverage of the membrane Fig. 2(b); although the filaments are too short to decide from these images which of the two SLB configurations in Fig. 3(a) and (b) is closer to the experimental observation. In the snapshots (c)–(f) we present different aggregates formed in MC simulations with $N = 1200$ monomers on a 473×507 lattice using different sets of interaction parameters. The mean protein coverage is about one monomer per 400 nm^2, but in all these cases the system presents a strong first order transition, with most of the protein condensed in a cluster, formed by a dense monolayer (about 20 nm^2 per monomer), while the rest of the simulation box contains a very rare 2D vapour made of monomers or very short filaments. The characteristics of the interactions between monomers (leading to flexible filaments, with spontaneous curvature and the presence of SLB) are shown in the polymorphism of the clusters. The O-cluster in (c) is similar to those observed in MC simulations without SLB and in the experimental results for FtsZ on mica.[15] New features are observed in the variants and combinations of the I-clusters (d and e) that take advantage of the SLB. The polymorphism induced by the SLB may be understood in simple geometrical terms. The shape in Fig. 2(e) is an adaptation of the I clusters to take advantage of the strong lateral bonds by taking rhombic, rather than rectangular shapes, so that the side with the filament ends becomes covered by strong lateral bonds with a filament, or narrow bundle. The filaments may also be broken inside the cluster, so that they meet the end with the correct orientation to form strong lateral bonds with the cover-bundle. The cluster in Fig. 2(d) is still another variant, in which the band of strong lateral contacts becomes enclosed in the cluster.

The relative free energy of these variant I forms depends on the interaction parameters, and on the size of the cluster. Large aggregates form tessellar combinations, similar to that in Fig. 2(g), with different clusters joined together in specific orientations. The AFM images in Fig. 2(f) and (h) are taken with the FtsZ mutant Cys2 on a bilayer with 90% *E. coli* polar lipids and 10% DSPE-Mal. The image (f) shows a bundle covering the open ends of the filaments, as in the MC snapshot (e), while the AFM image (h) is qualitatively similar to the patched pattern in (g). Notice that in these clusters the filaments do not show their spontaneous curvature, so that we cannot infer from the AFM images whether the SLB for this FtsZ mutant is better described by (a) or (b) alternatives in Fig. 3.

As in other LP systems,[23] the specific branching induced by the SLB produces a still higher level of meta-aggregates and LP networks. Increasing the protein coverage, with $N = 3598$ monomers over the same lattice size (which represents about 20% of the packed monolayer density), we found the structures presented in Fig. 4, in which the spontaneous curvature of the filaments and the specific angles given by the SLBs induce a rich variety of meta-cluster structures. In this case we keep the interaction parameters near the choice used in Fig. 1, only with a small decrease in the isotropic attraction to $\beta U_a = 1$ in panels (a) and (b), which is reflected in the formation of some short filaments or small clusters separated from the main cluster that includes nearly all the protein. In panel (c) with the same value $\beta U_a = 1.25$ as used in Fig. 1, the number of monomers away from the main cluster is already marginal. The shape of that cluster is determined by how the filament ends in C-clusters may form SLBs with the external filaments in other C-clusters, as shown in the snapshot (a1), while closed O shapes would be less effectively clustered, since they have less (or none) filament ends to form SLB. The O-clusters, which were often seen in the AFM images of FtsZ adsorbed on mica,[11] become rare when the protein is anchored to the bilayer membrane in a specific orientation. Instead, the FtsZ filaments form C-metaclusters like those in Fig. 1. Moreover, our MC simulation results show that the filaments may be aggregated in other possible forms, in particular, in Fig. 4(a2) we observe a SLB-closed spiral shape, as an hybrid between C and O-clusters, and also strings of

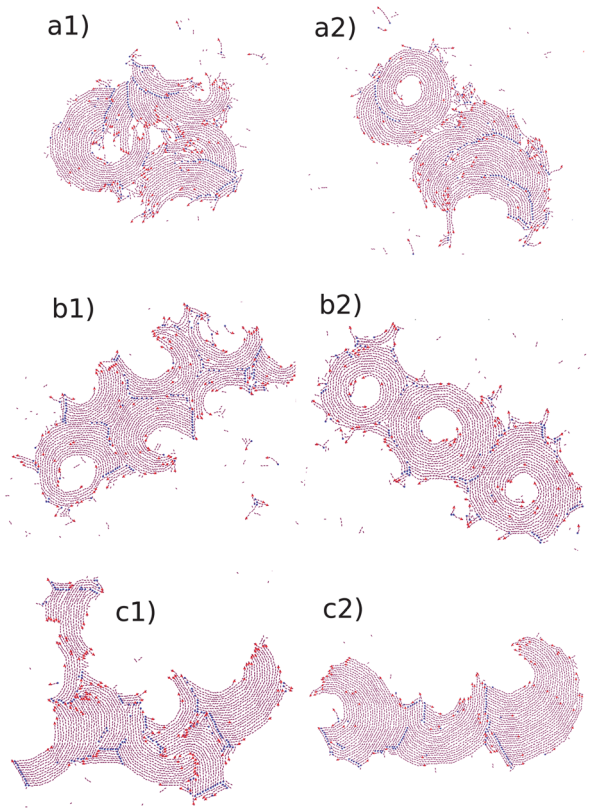

Fig. 4 Three pairs of complex aggregates formed by curved filaments. The images at the left correspond to an earlier stage of the simulation. For (a1) and (a2), the neighbour was required a relative angle of 60° to form SLB, while for (b) and (c) this angle was 120°, as depicted in Fig. 1. The isotropic lateral attraction was lowered to $U_a = 1$ for sets (a1) and (a2) and (b1) and (b2), while for sets (c1) and (c2) we keep all the model interaction parameters as in Fig. 1.

O-clusters, wedged by short external filaments Fig. 4(b2). That polymorphism induces a strong sensitivity to the details of the interactions in the model. The snapshot in Fig. 4(a) corresponds to the SLB topology in Fig. 3(a), while those in Fig. 4(b) and (c) correspond to the SLB in Fig. 3(b).

4 Slow time evolution and the relevance of the initial state

The computer simulation results offer a detailed view of the filament structures and we may quantify their characteristics beyond the resolution of the AFM images. In Table 1 we present some data from the MC simulations used to get the snapshots shown in Fig. 4. The angular configuration for the strong lateral bonds, and the strength of the isotropic lateral attraction produce important variations in the mean length of the filaments and in the number of SLBs. To give a full account of these changes we have to pay attention to the slow relaxation of these complex structures, typical of LP networks.[23] The left and right columns in Fig. 4 present snapshots taken at different times along the same MC simulations, always initialized with random distributions of monomers. The nucleation and growth of short filaments was enhanced by their aggregation in C-clusters and meta-clusters, as observed in the snapshots (a1), (b1) and (c1), taken after 32×10^6 MC steps. The late-time evolution of these structures is much slower, since it requires the inversion of the tail-to-head orientation of some filaments to reach the common curvature characteristic of C and O clusters. This process cannot be easily achieved by reptation moves, and it is usually achieved through rare fragmentation events. Snapshots (a2), (b2) and (c2) obtained after 160×10^6 MC steps show different possible trends in the late stages of these structures. In the time evolution of the experimental AFM images changes of similar characteristics appear over a time scale of hours, while the biological cycle for the formation of the *Z*-ring occurs in a scale of minutes, with a total number of protein monomers per cell similar to that ($N = 3598$) used in our simulations. Therefore, the typical shapes of the protein aggregates during their time evolution may be biologically more relevant than their truly equilibrated configurations, which would be observed only after times which are too long compared with the cell cycle.

For all the interaction parameters explored in Fig. 4 and Table 1, we observe that the total number of filaments decreases, and their mean length increases with time. The number of SLBs is very sensitive to small changes of the interaction parameters. In (a2), as some nested C-clusters evolve towards a closed-spiral, the total number of filaments decreases, and their mean length increases, but still keeping more than 80% of the filaments with a SLB. The change to the SLB angle in (b1) and (b2) produced longer filaments than in (a1) and (a2), but a smaller fraction of them form SLB in the back-to-back C-clusters in (b1), and this fraction decreases further in the string of O-clusters formed at later times (b2). As was already observed in the absence of SLBs, the balance between O and C shapes may be shifted towards the later by increasing the (weak) lateral attractions, as done between the systems in Fig. 4(b2) and (c2). The snapshots (c1) and (c2) show apparently similar C-clusters at early and late times, but the data presented in Table 1 prove that there is still a slow evolution in the structure of the aggregates, with the decay in the fraction of SLB per filament and the increase in the mean filament length. Notice that the SLB involve a small fraction of the monomers, between 10% and 5% of the total protein number, but these bonds are still determinant for the global aspect of the meta-aggregates.

The slow evolution of the filament clusters with time induces a strong sensitivity to the initial system. All the simulations in Fig. 4 evolved from a diluted random distribution of monomers. As in the simulations without SLB,[15] the early stages of the condensation leading to the snapshots shown in Fig. 4 are driven by the formation of short filaments, which become increasingly longer as the clusters grow. The late time structures are formed by coalescence and competition of clusters, with the transfer and sharing of filaments. The globally round shape of the cluster in the experimental AFM images in Fig. 1(a) contrasts with the band-like structures in Fig. 4. The experimental procedure used to obtain the AFM image in Fig. 1(a) and (c) was to attach the FtsZ protein to the bilayer membrane in the absence of the polymerizing agent GTP in the buffer, so that the tendency to form filaments is severely reduced, but there is still a tendency to condensate the protein in a 2D drop, under the action of the isotropic and strong lateral bonds. When GTP is added to the buffer, the filaments are rapidly formed within the pre-condensed protein drop, and that creates the characteristic shapes of the aggregates in Fig. 1(a) and (c).

In our computer simulations we may mimic that effect using MC equilibration runs with $U_b = 0$. We observe the condensation of a 2D drop under the effects of the lateral interactions. The filaments were only formed when U_b was turned on (to mimic that GTP was added in the experiment). That produces the globally round shapes in Fig. 1(b) and (d), in contrast with the more asymmetrical structures in Fig. 4. This malleability of the condensed forms, so that small changes in the interaction parameters, or even in the initial conditions, may produce important changes in the global structure, was associated with a relatively narrow range of values.[15] The biological tuning of FtsZ to get this malleability is probably associated with the biological function of the protein that has to be induced, through weak biochemical signals, to form (and to dissolve) the global structure of the septal ring, at the central position on the bacterial membrane, and at the correct time in the cell cycle.[4,6]

The difference between the snapshots in Fig. 1(b) and (d) is induced by the topology of SLB shown in the insets of that figure and in the sketch in Fig. 3. The number of these bonds is relatively small, but still their configuration is crucial to produce the back-to-back aggregation of C-clusters observed in Fig. 1(d) and 4(b) and (c). The opposite choice for the SLB would promote the nested C-clusters observed in Fig. 1(b) and 4(a1) and (a2). The experimental AFM image Fig. 1(c), taken with FtsZ mutant Cys255 on 90% *E. coli* Polar Extract and 10% DSPE-Mal, presents smooth concavities in the perimeter of the cluster, separated by pointed regions, and it is clearly associated with the SLB configuration (d) in Fig. 3 so that through the observation of the cluster shapes we are able to discern details of the

preferred branching in the interaction between monomers anchored to the membrane at the 255 position. The shape of the cluster in Fig. 1(a), taken with the FtsZ mutant Cys2 on the same membrane, is very different of that with the Cys255 mutant, and it may be considered to be much similar to the MC snapshot (b), obtained with the configuration (a) for the SLB in Fig. 3.

Notice that the experimental AFM images in Fig. 1 are very characteristic aggregates observed under the new biomimetic conditions explored in the recent experiments,[14] with specific anchoring of the protein on a lipid bilayer. The structures are very different from those observed when the protein is directly absorbed on mica, in which there is no evidence of branching filaments, probably because the preferential orientation of the protein monomers on the substrate is more loosely defined, and the specific interactions leading to the SLB observed here become smeared into the isotropic lateral attraction. It is also relevant that the experimental results with different FtsZ mutants, *i.e.* with opposite orientations of the protein monomers on the lipid bilayer, may be correlated with the patterns observed in MC simulations with the alternative configurations of the SLB in our model.

The polymorphism of the self-assembled structures induces strong sensitivity to the details of the interactions in the model, which may be tuned to reproduce the AFM images under different experimental conditions. When we use these comparisons to identify the relevant interactions between protein monomers we have to consider the very slow relaxation of the cluster shapes, so that even after long equilibration times, the global form of the aggregates reflects the process in which it was built, discriminating between a polymerization induced in a condensed drop *versus* the simultaneous polymerization–condensation from isolated monomers. In this respect, it is interesting that the AFM patterns in Fig. 1 are observed only when the protein mutant (either FtsZ mutant Cys2 or C255) is anchored on bilayer membranes formed by the phospholipid mixture of the *E. coli* membrane, and not on the simpler synthetic DOPC membranes. The interpretation from our results is that the negative character of the *E. coli* lipids and/or the segregation of the different lipid molecules help us to produce the condensation of the FtsZ drop, even in the absence of the polymerizing agent GTP.

5 Concluding remarks

We have used a statistical physics approach to study the complex structures and patterns formed by the bacterial protein FtsZ under a specific anchoring on a lipid bilayer that produces strong trimer bonds between the protein monomers and branched filaments. A lattice model with a few parameters describing the interactions between the protein monomers may be tuned to reproduce the features observed in the experimental AFM images. We can clearly discern not only the global effects of filament branching, but even the subtle differences between the two alternative choices for the coupling between branching and spontaneous curvature, shown in Fig. 3. It is only through the collective behaviour of these living polymers that such effects are amplified and produce globally different structures. In contrast to the molecular structure strategy, we do not aim at a detailed (atomistic) view of proteins, but we try to simplify their interactions as much as possible, while preserving their observable effects. As demonstrated in this paper, the new scanning microscopy techniques offer the experimental data and images needed to tune the simplified models. Following a well-beaten path in soft-matter physics, we aim at the convergence between the molecular (bottom-up) and the statistical (top-down) approaches. The first one should provide the *atomistic origin* for the effective parameters used by the second, while the later discloses the *relevant part* of the complex protein structure.

With respect to the specific protein studied here, FtsZ, we have found that its interactions are finely tuned to achieve an amazing polymorphism. Minor changes in the interaction parameters, or just in the condensation history, produce qualitative changes in the self-assembled structures, which is probably relevant to its biological function.[24] The presence of trimeric (SLB) interactions may be relevant both for the early and late time states in the formation of the aggregates, first as an enhancement for protein condensation, even in the absence of polymerization, and then as a bias towards the formation of characteristic meta-aggregates. We have to point out that the results presented here correspond to a specific and tight orientation of the protein on the membrane. AFM images with the protein anchored in different positions, or under a looser attachment of the protein to the substrate, show different structures. As a soft-matter system, FtsZ anchored to bilayer membranes offers an interesting living-polymer system, accessible to experimental studies, and with tunable interactions through the design of artificial mutants that may be anchored in specific orientations. The comparison between the experimental AFM images and the results for simple models helps us to understand the link between the molecular interactions and the complex polymorphism of the self-assembled structures.

Acknowledgements

We are grateful to German Rivas for providing the FtsZ mutant used for the AFM images and Alfonso Paez for the code of the lattice model in ref. 15. PGdPS has done this work as a holder of FPU grant from the Ministerio de Educación of Spain. We acknowledge financial support from the Comunidad de Madrid, through projects NOBIMAT-M S2OO9/MAT-1507 and MODELICO-S2009/ESP-1691, and from the Ministerio de Ciencia e Innovación of Spain, through projects Plan Nacional BIO2008-04478-C03-00, FIS2010-22047-C05-01 and CONSOLIDER INGENIO 2010 CSD2007-00010 and DIVINOCELL FP7 HEALTH-F3-2009-223431 (European Commission to MVe).

References

1 E. Callaway, *Nature*, 2008, **451**, 124–126.
2 L. Romberg and P. Levin, *Annu. Rev. Microbiol.*, 2003, **57**, 157.
3 A. Dajkovic and J. Lutkenhaus, *J. Mol. Microbiol. Biotechnol.*, 2006, **11**, 140.
4 M. Vicente and A. I. Rico, *Mol. Microbiol.*, 2006, **61**, 5.

5 D. J. Haydon, N. R. Stokes, R. Ure, G. Galbraith, J. M. Bennett, D. R. Brown, P. J. Baker, V. V. Barynin, D. W. Rice, S. E. Sedelnikova, J. R. Heal, J. M. Sheridan, S. T. Aiwale, P. K. Chauhan, A. Srivastava, A. Taneja, I. Collins, J. Errington and L. G. Czaplewski, *Science*, 2008, **321**, 1673–1675.
6 J. Mingorance, G. Rivas, M. Vélez, P. Gómez-Puertas and M. Vicente, *Trends Microbiol.*, 2010, **18**, 348356.
7 M. Szwarc, *Nature*, 1956, **178**, 1168.
8 M. Cates, *Macromolecules*, 1987, **20**, 2289.
9 T. F. A. D. Greef, M. M. J. Smulders, M. Wolffs, A. P. H. J. Schenning, R. P. Sijbesma and E. W. Meijer, *Chem. Rev.*, 2009, **109**, 5687–5754.
10 J. Mingorance, M. Tadros, M. Vicente, J. M. González, G. Rivas and M. Vélez, *J. Biol. Chem.*, 2005, **280**, 20909–20914.
11 I. Hörger, E. Velasco, J. Mingorance, G. Rivas, P. Tarazona and M. Vélez, *Phys. Rev. E: Stat., Nonlinear, Soft Matter Phys.*, 2008, **77**, 011902.
12 I. H. I. Hörger, E. Velasco, G. Rivas, M. Vélez and P. Tarazona, *Biophys. J.*, 2008, **94**, L81–L83.
13 P. Mateos-Gil, I. Márquez, P. López-Navajas, M. Jiménez, M. Vicente, J. Mingorance, G. Rivas and M. Vélez, *Biochim. Biophys. Acta, Biomembr.*, 2012, **1818**, 806.
14 M. Encinar, *et al.*, *Langmuir*, 2013, to be published.
15 A. Paez, P. Tarazona, P. Mateos-Gil and M. Vélez, *Soft Matter*, 2009, **5**, 2625–2637.
16 A. Dajkovic, G. Lan, S. X. Sun, D. Wirtz and J. Lutkenhaus, *Curr. Biol.*, 2008, **18**, 235–244.
17 G. Lan, B. R. Daniels, T. M. Dobrowsky, D. Wirtz and S. X. Sun, *Proc. Natl. Acad. Sci. U. S. A.*, 2009, **106**, 121.
18 B. Ghosh and A. Sain, *Phys. Rev. Lett.*, 2008, **101**, 178101.
19 J. L. Löwe and L. A. Amos, *Nature*, 1998, **391**, 203–206.
20 F. Moreno-Herrero, P. dePablo, R. Fernández-Sánchez, R. Colchero, J. Gómez-Herrero and A. Baró, *Appl. Phys. Lett.*, 2002, **1**, 2620–2622.
21 M. Sayar and S. I. Stupp, *Phys. Rev. E: Stat., Nonlinear, Soft Matter Phys.*, 2005, **72**, 011803.
22 P. Mateos-Gil, A. Paez, I. Hörger, G. Rivas, M. Vicente, P. Tarazona and M. Vélez, *Proc. Natl. Acad. Sci. U. S. A.*, 2012, **109**, 8133–8138.
23 T. Drye and M. Cates, *J. Chem. Phys.*, 1992, **96**, 1367.
24 A. Paez, P. Mateos-Gil, I. Hörger, J. Mingorance, G. Rivas, M. Vicente, M. Vélez and P. Tarazona, *PMC Biophys.*, 2009, **9**, 8.